Quantum theory of optical temporal phase and instantaneous frequency

Mankei Tsang,[1,*] Jeffrey H. Shapiro,[1] and Seth Lloyd[1,2]
[1]*Research Laboratory of Electronics, Massachusetts Institute of Technology, Cambridge, Massachusetts 02139, USA*
[2]*Department of Mechanical Engineering, Massachusetts Institute of Technology, Cambridge, Massachusetts 02139, USA*
(Received 3 April 2008; revised manuscript received 4 September 2008; published 18 November 2008)

We propose a general quantum theory of optical phase and instantaneous frequency in the time domain for slowly varying optical signals. Guided by classical estimation theory, we design homodyne phase-locked loops that enable quantum-limited measurements of temporal phase and instantaneous frequency. Standard and Heisenberg quantum limits to such measurements are then derived. For optical sensing applications, we propose multipass and Fabry-Pérot position and velocity sensors that take advantage of the signal-to-noise-ratio enhancement effect of wide-band angle modulation without requiring nonclassical light. We also generalize our theory to three spatial dimensions for nonrelativistic bosons and define a Hermitian fluid velocity operator, which provides a theoretical underpinning to the current-algebra approach of quantum hydrodynamics.

DOI: 10.1103/PhysRevA.78.053820 PACS number(s): 42.50.Ct, 42.79.Qx, 03.75.Kk, 47.37.+q

I. INTRODUCTION

Frequency modulation (FM) radio sounds better than amplitude modulation (AM) radio, because by encoding a message in the instantaneous frequency, defined as the rate of change of the signal phase, FM uses more transmission bandwidth to improve the signal-to-noise ratio (SNR) [1–3]. In optical communications, FM and phase modulation (PM) techniques have also received significant attention and can offer higher SNRs in photonic links than standard intensity modulation [4]. Quantum statistics is expected to play a major role in the performance of coherent optical communication systems [5–7], but although a treatment of digital FM quantum noise was briefly mentioned by Yuen [7], a more fundamental quantum theory of temporal phase and instantaneous frequency is not yet available. In optical sensing, on the other hand, a considerable amount of research has been devoted to the study of ultimate quantum limits to phase [8–11] and velocity [12] measurements. A quantum description of temporal phase and instantaneous frequency is again needed to deal with any rapid change in the measured parameters. For example, in laser Doppler velocimetry, which has been widely used in fluid dynamics [13] and blood flow diagnostics [14], the velocity of the interrogated sample actually shifts the instantaneous frequency of the reflected optical signal and not the average frequency directly, so the quantum limits to velocity measurements derived in Ref. [12] are no longer accurate when the velocity changes rapidly.

A rigorous quantum description of the optical phase is, unfortunately, not trivial even for one optical mode, and has been a subject of long-running debate [9,15–21] since the issue was first raised by Dirac at the birth of quantum electrodynamics [22]. The difficulty of defining a phase operator is shared by the superfluid and Bose-Einstein condensate community [23], where the fluid velocity in Landau's formulation of quantum hydrodynamics [24] is often related to the phase gradient of an order parameter. Beyond the Bogoliubov approximation, while Landau has proposed a fluid velocity operator [24], many have argued against its existence [25].

In this paper, we show how the temporal phase and the instantaneous frequency of a slowly varying optical signal can be treated consistently in the quantum regime. By limiting the bandwidth of the optical Hilbert space, we discretize the continuous time domain into orthogonal "wave-packet" modes via the sampling theorem. This crucial step allows us to apply previous studies of discrete-mode quantum phase to the time domain. To enable quantum-limited temporal-phase measurements in practice, we use estimation theory to design homodyne phase-locked-loop measurement schemes, similar to adaptive phase measurements [27–29]. Standard and Heisenberg quantum limits to the accuracy of temporal-phase and instantaneous-frequency measurements for coherent states and squeezed states are then derived. For sensing applications, we propose multipass and Fabry-Pérot position and velocity sensors that take advantage of the SNR enhancement effect of wideband angle modulation. Finally, we generalize our time-domain formalism for optics to three spatial dimensions for nonrelativistic bosons and define a Hermitian fluid velocity operator, which provides a theoretical underpinning for the current-algebra approach to quantum hydrodynamics [23–26].

II. QUANTIZATION OF BAND-LIMITED OPTICAL FIELDS

To describe a typical free-space or fiber optical experiment, propagating modes are usually quantized in terms of the frequency, transverse momentum, and polarization degrees of freedom [6,30,31]. We shall consider a plane wave of a certain polarization in free space or one fiber mode at an observation plane along the optical axis, and allow only the frequency degree of freedom for simplicity. In the slowly varying envelope regime, one can regard the optical fields as a one-dimensional nonrelativistic many-boson system and quantize accordingly [6,30–32]. The positive-frequency

*mankei@mit.edu

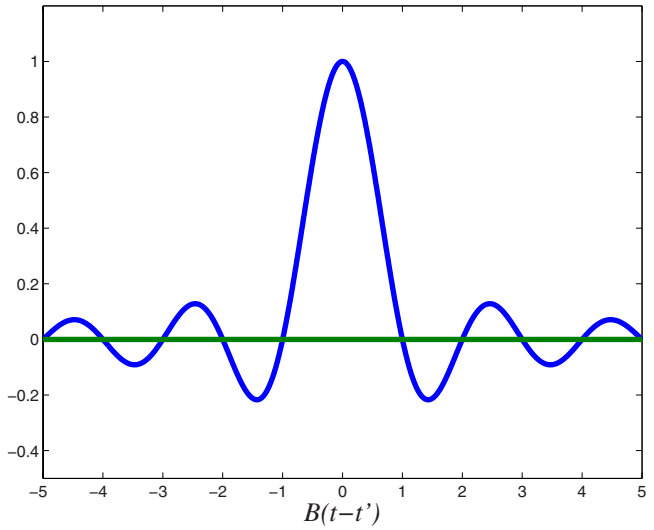

FIG. 1. (Color online) sinc $B(t-t')$.

electric-field operator can then be approximated as

$$\hat{E}^{(+)}(t) \propto \hat{A}(t)\exp(-i2\pi f_0 t), \tag{2.1}$$

where $\hat{A}(t)$ is the envelope annihilation operator and f_0 is the carrier optical frequency. We shall make the physically reasonable assumption that our ability to create, manipulate, transmit, and measure the optical fields is limited to a certain bandwidth B near the carrier optical frequency f_0. We can then express $\hat{A}(t)$ as the band-limited Fourier transform of the frequency-domain annihilation operator $\hat{a}(f)$,

$$\hat{A}(t) = \int_{-B/2}^{B/2} df \hat{a}(f)\exp(-i2\pi f t). \tag{2.2}$$

In other words, we only need the set of operators $\hat{a}(f)$ and $\hat{a}^\dagger(f)$ for which f falls within the band ($|f| < B/2$) to describe our experiments. To satisfy the slowly varying envelope approximation, we require $B/2 \ll f_0$. The commutation relation between $\hat{a}(f)$ and the corresponding creation operator $\hat{a}^\dagger(f)$ is

$$[\hat{a}(f), \hat{a}^\dagger(f')] = \delta(f-f'), \tag{2.3}$$

which leads to the following time-domain commutation relation:

$$[\hat{A}(t), \hat{A}^\dagger(t')] = B \text{ sinc } B(t-t'), \tag{2.4}$$

where the sinc function is defined as

$$\text{sinc}(x) \equiv \frac{\sin(\pi x)}{\pi x}. \tag{2.5}$$

We make the important observation that the time-domain commutator given by Eq. (2.4) goes to zero at discrete intervals, as shown in Fig. 1, when $t-t'$ is a nonzero-integer multiple of $1/B$. If we discretize time into such intervals, that is, let

$$t_j \equiv t_0 + j\delta t, \tag{2.6}$$

where j is an integer and

$$\delta t \equiv \frac{1}{B}, \tag{2.7}$$

the commutator at these sampled times becomes

$$[\hat{A}(t_j), \hat{A}^\dagger(t_k)] = B\delta_{jk} = \frac{\delta_{jk}}{\delta t}. \tag{2.8}$$

The sampled times have become orthogonal "wave-packet" modes, as described qualitatively but not substantiated in Ref. [5]. The operators can be renormalized to give the conventional discrete-mode commutator,

$$\hat{a}_j \equiv \hat{A}(t_j)\sqrt{\delta t}, \quad [\hat{a}_j, \hat{a}_k^\dagger] = \delta_{jk}, \tag{2.9}$$

and the continuous-time and continuous-frequency operators can be reconstructed using the sampling theorem,

$$\hat{A}(t) = \sqrt{B}\sum_{j=-\infty}^{\infty} \hat{a}_j \text{ sinc } B(t-t_j), \tag{2.10}$$

$$\hat{a}(f) = \frac{1}{\sqrt{B}}\sum_{j=-\infty}^{\infty} \hat{a}_j \exp(i2\pi f t_j) \quad \text{for } |f| < \frac{B}{2}. \tag{2.11}$$

By virtue of the sampling theorem, the use of the discrete-time operators on the band-limited Hilbert space is completely equivalent to the use of continuous-time or continuous-frequency operators.

The band-limited Hilbert space can be spanned by photon-number states in discrete wave-packet modes,

$$|n_j\rangle_j \equiv \frac{1}{\sqrt{n_j!}}(\hat{a}_j^\dagger)^{n_j}|0\rangle_j, \quad |\boldsymbol{n}\rangle \equiv \bigotimes_j |n_j\rangle_j, \tag{2.12}$$

$$\hat{\mathbf{1}} = \sum_{\boldsymbol{n}} |\boldsymbol{n}\rangle\langle\boldsymbol{n}|, \tag{2.13}$$

where n_j is the number of photons in the wave-packet mode at time t_j, and for convenience we use boldface $\boldsymbol{n}$ to denote the vector $\{\ldots, n_j, n_{j+1}, \ldots\}$. Appendix A lists other notations that we shall use to describe algebra in the discrete time domain. For a pure state $|\Psi\rangle$, the photon-number representation is

$$C[\boldsymbol{n}] \equiv \langle\boldsymbol{n}|\Psi\rangle, \quad \sum_{\boldsymbol{n}} |C[\boldsymbol{n}]|^2 = 1. \tag{2.14}$$

Another way of spanning the Hilbert space is via nonorthogonal multiphoton time-measurement eigenstates [19,31,32],

$$|\tau_1, \ldots, \tau_N\rangle \equiv \frac{1}{\sqrt{N!}}\hat{A}^\dagger(\tau_1)\cdots\hat{A}^\dagger(\tau_N)|0\rangle, \tag{2.15}$$

$$\hat{\mathbf{1}} = \sum_{N=0}^{\infty} \int d\tau_1 \ldots d\tau_N |\tau_1, \ldots, \tau_N\rangle\langle\tau_1, \ldots, \tau_N|. \tag{2.16}$$

The multiphoton wave function is then

$$\psi_N(\tau_1, \ldots, \tau_N) \equiv \langle\tau_1, \ldots, \tau_N|\Psi\rangle, \tag{2.17}$$

$$\sum_{N=0}^{\infty} \int d\tau_1 \cdots d\tau_N |\psi_N(\tau_1, \ldots, \tau_N)|^2 = 1, \quad (2.18)$$

which is related to the photon-number representation by [32]

$$\psi_N(\tau_1, \ldots, \tau_N) = \sum_{\boldsymbol{n}, \Sigma_j n_j = N} C[\boldsymbol{n}] \Phi_{\boldsymbol{n}}(\tau_1, \ldots, \tau_N), \quad (2.19)$$

$$\Phi_{\boldsymbol{n}}(\tau_1, \ldots, \tau_N) \equiv \left(\frac{\prod_j n_j!}{N! \, \delta t^N} \right)^{1/2} \sum_{l=1}^{N!} \prod_j \prod_{r_j = \Sigma_k^{j-1} n_k + 1}^{\Sigma_k^j n_k + n_j} \mathrm{sinc}\left(\frac{\tau_{P_l(r_j)} - t_j}{\delta t} \right), \quad (2.20)$$

where $P_l(r_j)$ is an element of a permutation of $\{r_1, \ldots, r_N\}$ and the sum over l is over all $N!$ possible permutations so that $\Phi_{\boldsymbol{n}}$ is symmetric. The inverse relation is

$$C[\boldsymbol{n}] = \left(\frac{N! \, \delta t^N}{\prod_j n_j!} \right)^{1/2} \psi_N(\ldots, \underbrace{t_j, \ldots, t_j}_{n_j \text{ terms}}, \underbrace{t_{j+1}, \ldots, t_{j+1}}_{n_{j+1} \text{ terms}}, \ldots), \quad (2.21)$$

where $N = \Sigma_j n_j$. For example, a coherent state can be defined in the continuous-time domain as

$$|\mathcal{A}(t)\rangle \equiv \exp\left[-\frac{\bar{N}}{2} + \int_{-\infty}^{\infty} dt \mathcal{A}(t) \hat{A}^\dagger(t) \right] |0\rangle, \quad (2.22)$$

$$\hat{A}(t)|\mathcal{A}(t)\rangle = \mathcal{A}(t)|\mathcal{A}(t)\rangle, \quad \bar{N} = \int_{-\infty}^{\infty} dt |\mathcal{A}(t)|^2, \quad (2.23)$$

where $\mathcal{A}(t)$ is a band-limited envelope function and $\bar{N}$ is the average photon number. In terms of the wave-function representation,

$$\psi_N(\tau_1, \ldots, \tau_N) = \frac{\exp(-\bar{N}/2)}{\sqrt{N!}} \mathcal{A}(\tau_1) \cdots \mathcal{A}(\tau_N). \quad (2.24)$$

Using Eq. (2.21), we obtain the photon-number representation for a coherent state,

$$C[\boldsymbol{n}] = \prod_j \frac{\exp(-|\alpha_j|^2/2)}{\sqrt{n_j!}} \alpha_j^{n_j}, \quad \alpha_j = \mathcal{A}(t_j)\sqrt{\delta t}, \quad (2.25)$$

which shows that any coherent state can be written as a collection of independent coherent states in wave-packet modes.

III. CANONICAL TEMPORAL-PHASE MEASUREMENTS

For each wave-packet mode at time t_j, we can define the nonunitary Susskind-Glogower exponential-phase operator [15] as

$$\hat{\mathcal{E}}_j \equiv \frac{1}{\sqrt{\hat{a}_j \hat{a}_j^\dagger}} \hat{a}_j = \frac{1}{\sqrt{\hat{A}(t_j)\hat{A}^\dagger(t_j)}} \hat{A}(t_j). \quad (3.1)$$

Since $\hat{\mathcal{E}}_j$ depends only on the field operators at time t_j, it can be regarded as an instantaneous phase operator. Despite the nonunitary nature of $\hat{\mathcal{E}}_j$, its eigenstates form a nonorthogonal basis of the Hilbert space,

$$|\boldsymbol{\phi}\rangle \equiv \sum_{\boldsymbol{n}} \exp(i\boldsymbol{n} \cdot \boldsymbol{\phi}) |\boldsymbol{n}\rangle, \quad \boldsymbol{\phi}_0 \leqslant \boldsymbol{\phi} < \boldsymbol{\phi}_0 + 2\pi, \quad (3.2)$$

$$\hat{\mathbf{1}} = \int D\boldsymbol{\phi} |\boldsymbol{\phi}\rangle\langle\boldsymbol{\phi}|, \quad D\boldsymbol{\phi} \equiv \prod_j \frac{d\phi_j}{2\pi}. \quad (3.3)$$

The Susskind-Glogower eigenstates can thus be used to define a temporal-phase positive operator-valued measure (POVM), also called a probability operator measure (POM) [9,20,21],

$$\hat{\Pi}[\boldsymbol{\phi}] \equiv |\boldsymbol{\phi}\rangle\langle\boldsymbol{\phi}|, \quad \int D\boldsymbol{\phi} \hat{\Pi}[\boldsymbol{\phi}] = \hat{\mathbf{1}}, \quad (3.4)$$

which corresponds to a measurement of instantantaneous optical phases $\{\ldots, \phi_j, \phi_{j+1}, \ldots\}$ at times $\{\ldots, t_j, t_{j+1}, \ldots\}$. It can be shown, by generalizing the single-mode treatment in Ref. [21], that the POVM given by Eq. (3.4) corresponds to the optimal temporal-phase measurements for any periodic cost function with non-negative Fourier coefficients. Following Leonhardt *et al.* [18], we shall refer to the phase POVM measurement as the canonical phase measurement. In the single-mode case, an experimental canonical phase measurement scheme has been proposed by Pregnell and Pegg [33]. While generalization of their scheme to the time domain is conceivable, it is beyond the scope of this paper to investigate experimental canonical temporal-phase measurement schemes in detail.

The canonical temporal-phase probability density is

$$p[\boldsymbol{\phi}] \equiv \mathrm{Tr}\{\hat{\rho}\hat{\Pi}[\boldsymbol{\phi}]\}, \quad \int D\boldsymbol{\phi} p[\boldsymbol{\phi}] = 1. \quad (3.5)$$

For a pure state, one can define a temporal-phase representation as the discrete Fourier transform of the photon-number representation,

$$\mathcal{C}[\boldsymbol{\phi}] \equiv \langle\boldsymbol{\phi}|\Psi\rangle = \sum_{\boldsymbol{n}} \exp(-i\boldsymbol{n} \cdot \boldsymbol{\phi}) C[\boldsymbol{n}], \quad (3.6)$$

the magnitude squared of which gives the probability density $p(\boldsymbol{\phi})$.

One can also extend the Pegg-Barnett formalism to the time domain by considering a Hilbert space spanned by finite-photon-number states $|\boldsymbol{n}\rangle$ with $\mathbf{0} \leqslant \boldsymbol{n} \leqslant \boldsymbol{s}$. The commutator for $\hat{a}_j$ and $\hat{a}_j^\dagger$ becomes

$$[\hat{a}_j, \hat{a}_k^\dagger] = \delta_{jk}[1 - (s_j + 1)|s_j\rangle_j\langle s_j|], \quad (3.7)$$

although applying the commutator to physical states in the $s_j \to \infty$ limit recovers the usual commutator $[\hat{a}_j, \hat{a}_k^\dagger]_p = \delta_{jk}$. A unitary Pegg-Barnett exponential-phase operator can be defined in the photon-number basis as

$$\exp(i\hat{\phi}_j) \equiv \sum_{n_j=1}^{s_j} |n_j - 1\rangle_j\langle n_j| + \exp[i(s_j+1)\phi_{0j}]|s_j\rangle_j\langle 0|. \tag{3.8}$$

By taking the limit $s_j \to \infty$ at the end of calculations, the Pegg-Barnett theory predicts the same phase statistics as the canonical phase statistics governed by Eq. (3.5), and the two theories can be regarded as equivalent and complementary [9].

To define an instantaneous-frequency operator, consider the classical definition

$$F(t) \equiv -\frac{1}{2\pi}\frac{d}{dt}\phi(t). \tag{3.9}$$

$\phi(t)$ can be multivalued or even undefined when the intensity is zero, so to avoid this ambiguity we write the instantaneous frequency in terms of $\exp[i\phi(t)]$,

$$\begin{aligned} F(t) &= \frac{1}{4\pi i}\left\{\exp[i\phi(t)]\frac{d}{dt}\exp[-i\phi(t)] - \text{c.c.}\right\} \\ &= \frac{1}{2\pi}\frac{d}{dt'}\sin[\phi(t)-\phi(t')]\Big|_{t'=t}, \end{aligned} \tag{3.10}$$

where c.c. denotes complex conjugate. In the quantum regime, we can discretize $F(t)$ and express it exactly in terms of the Pegg-Barnett operator,

$$\hat{F}_j = \frac{1}{2\pi\delta t}\sum_k d_{j-k}\sin(\hat{\phi}_j - \hat{\phi}_k), \tag{3.11}$$

$$\sin(\hat{\phi}_j - \hat{\phi}_k) = \frac{1}{2i}[\exp(i\hat{\phi}_j - i\hat{\phi}_k) - \text{H.c.}]. \tag{3.12}$$

H.c. denotes Hermitian conjugate, and d_{j-k} is called the differentiator [34], the discrete impulse response that corresponds to differentiation,

$$d_{j-k} = \begin{cases} (-1)^{j-k}/(j-k), & j \neq k, \\ 0, & j = k. \end{cases} \tag{3.13}$$

$\hat{F}_j$ is Hermitian and well defined in the finite-photon-number band-limited Hilbert space, but given the difficulty of canonical phase measurements in practice, it might be even more difficult to measure the instantaneous-frequency operator, unless approximations are made.

IV. MAXIMUM A POSTERIORI ESTIMATION

It is difficult to perform canonical phase measurements, and first-order field measurements, such as homodyne detection and heterodyne detection, are often preferred in practice. Statistics of heterodyne detection and its variants [17] are governed by the Q distribution [18,35–37], which is broader than the Wigner distribution that governs homodyne detection [35,36], so ideally one would like to use only homodyne detection to measure the phase and instantaneous frequency. In this section, we would like to show how this can be done from the perspective of estimation theory, which naturally leads to the use of homodyne phase-locked loops to perform angle demodulation.

The Wigner distribution is defined as [36]

$$W[\boldsymbol{x},\boldsymbol{y}] \equiv \int D\boldsymbol{b}\,\exp(\boldsymbol{b}^*\cdot\boldsymbol{a} - \boldsymbol{b}\cdot\boldsymbol{a}^*)\chi[\boldsymbol{b}], \tag{4.1}$$

$$D\boldsymbol{b} \equiv \prod_j \frac{d^2 b_j}{\pi^2}, \quad \boldsymbol{a} \equiv \frac{1}{2}(\boldsymbol{x}+i\boldsymbol{y}), \tag{4.2}$$

$$\chi[\boldsymbol{b}] \equiv \text{Tr}\{\hat{\rho}\exp(\boldsymbol{b}\cdot\hat{\boldsymbol{a}}^\dagger - \boldsymbol{b}^*\cdot\hat{\boldsymbol{a}})\}, \tag{4.3}$$

which governs the statistics of operators that can be expressed in Weyl-ordered quadrature operators [19,36],

$$\langle f^{(W)}[\hat{\boldsymbol{x}},\hat{\boldsymbol{y}}]\rangle = \int D\boldsymbol{x}D\boldsymbol{y} f[\boldsymbol{x},\boldsymbol{y}]W[\boldsymbol{x},\boldsymbol{y}], \tag{4.4}$$

$$\hat{\boldsymbol{x}} \equiv \hat{\boldsymbol{a}} + \hat{\boldsymbol{a}}^\dagger, \quad \hat{\boldsymbol{y}} \equiv -i(\hat{\boldsymbol{a}} - \hat{\boldsymbol{a}}^\dagger), \tag{4.5}$$

$$D\boldsymbol{x}D\boldsymbol{y} \equiv \prod_j dx_j dy_j, \tag{4.6}$$

where the superscript (W) denotes Weyl ordering. In the following, we shall consider only quantum states that have nonnegative Wigner distributions, and assume that measurements of Weyl-ordered quadrature operators can always be realized. The Wigner distribution is then a qualified classical probability distribution that we can use in classical estimation theory.

If the range of phase modulation exceeds 2π, one must unwrap the measured phase to unambiguously decode the message contained within. Phase unwrapping can be done only if one has *a priori* information about the message, because otherwise one would have no other way to distinguish ϕ_j from $\phi_j + 2n\pi$, n being an arbitrary integer, in a measurement. To incorporate *a priori* information in angle demodulation, we shall use maximum *a posteriori* (MAP) estimation [1,2]. Given an *a priori* probability distribution of the message $P[\boldsymbol{m}] = P(\ldots, m_j, m_{j+1}, \ldots)$, MAP estimation seeks the message that maximizes the *a posteriori* probability distribution

$$P[\boldsymbol{m}|\boldsymbol{x},\boldsymbol{y}] = \frac{W[\boldsymbol{x},\boldsymbol{y}|\boldsymbol{m}]P[\boldsymbol{m}]}{P[\boldsymbol{x},\boldsymbol{y}]} \tag{4.7}$$

for a set of measurements in terms of $\boldsymbol{x}$ and $\boldsymbol{y}$, and is asymptotically efficient. Taking the logarithm of the *a posteriori* distribution and differentiating with respect to $\boldsymbol{m}$, we arrive at the vectorial MAP equation, the solution of which gives the MAP estimate $\tilde{\boldsymbol{m}}$,

$$(\nabla_{\boldsymbol{m}} \ln W[\boldsymbol{x},\boldsymbol{y}|\boldsymbol{m}] + \nabla_{\boldsymbol{m}} \ln P[\boldsymbol{m}])_{\boldsymbol{m}=\tilde{\boldsymbol{m}}} = \boldsymbol{0}, \tag{4.8}$$

where the gradient operator $\nabla_{\boldsymbol{m}}$ is defined as

$$\nabla_{\boldsymbol{m}} \equiv \left\{\ldots, \frac{\partial}{\partial m_j}, \frac{\partial}{\partial m_{j+1}}, \ldots\right\}. \tag{4.9}$$

The MAP equation (4.8) can be significantly simplified if the probability distributions are Gaussian. We therefore model

the message $\boldsymbol{m}$ as a zero-mean Gaussian random process,

$$P[\boldsymbol{m}] \propto \exp\left(-\frac{1}{2}\boldsymbol{m}\cdot\boldsymbol{K}_m^{-1}\cdot\boldsymbol{m}\right), \tag{4.10}$$

$$\boldsymbol{K}_m \equiv \langle \Delta\boldsymbol{m}\otimes\Delta\boldsymbol{m}\rangle, \tag{4.11}$$

where $\boldsymbol{K}_m$ is the message covariance matrix. In angle modulation systems, the mean phase is a linear transformation of the message,

$$\bar{\boldsymbol{\phi}} = \boldsymbol{H}\cdot\boldsymbol{m}, \tag{4.12}$$

where $\boldsymbol{H}$ is a real impulse response. For example, the impulse response for PM is

$$\boldsymbol{H} = \beta\boldsymbol{I}, \tag{4.13}$$

where β is called the modulation index and $\boldsymbol{I}$ is the identity matrix, and the impulse response for FM is

$$H_{jk} = -2\pi\mathcal{F}\int_{-\infty}^{t_j} dt\ \mathrm{sinc}\ B(t-t_k), \tag{4.14}$$

where $\mathcal{F}$ is called the frequency deviation. Although the Wigner distribution is Gaussian for squeezed states [36], we shall first study the simpler coherent states.

A. Coherent states

To derive the Wigner distribution for a coherent state, let us start with that for the vacuum,

$$W_0[\boldsymbol{x}_0,\boldsymbol{y}_0] \propto \exp\left(-\frac{1}{2}\boldsymbol{x}_0\cdot\boldsymbol{x}_0 - \frac{1}{2}\boldsymbol{y}_0\cdot\boldsymbol{y}_0\right). \tag{4.15}$$

A coherent state with mean phase $\bar{\boldsymbol{\phi}}$ and constant mean amplitude $|\alpha|$ is obtained by displacing the vacuum along the $\boldsymbol{x}_0$ quadrature followed by phase modulation. The resulting Wigner distribution is

$$W[\boldsymbol{x},\boldsymbol{y}|\bar{\boldsymbol{\phi}}] = W_0[\boldsymbol{x}_0[\boldsymbol{x},\boldsymbol{y}],\boldsymbol{y}_0[\boldsymbol{x},\boldsymbol{y}]], \tag{4.16}$$

$$\boldsymbol{x}_0 = \boldsymbol{x}\cos\bar{\boldsymbol{\phi}} + \boldsymbol{y}\sin\bar{\boldsymbol{\phi}} - 2|\alpha|, \tag{4.17}$$

$$\boldsymbol{y}_0 = -\boldsymbol{x}\sin\bar{\boldsymbol{\phi}} + \boldsymbol{y}\cos\bar{\boldsymbol{\phi}}, \tag{4.18}$$

which can be used as the conditional distribution in the MAP equation (4.8). After some algebra, the MAP equation becomes

$$\tilde{\boldsymbol{m}} = 2|\alpha|\boldsymbol{K}_m\cdot\boldsymbol{H}^T\cdot\boldsymbol{p}, \tag{4.19}$$

where $\boldsymbol{p}$ is a quadrature field that depends linearly on the complex field $\boldsymbol{a}$ and nonlinearly on the estimated message $\tilde{\boldsymbol{m}}$,

$$\boldsymbol{p} \equiv -i[\boldsymbol{a}\exp(-i\tilde{\boldsymbol{\phi}}) - \boldsymbol{a}^*\exp(i\tilde{\boldsymbol{\phi}})], \quad \tilde{\boldsymbol{\phi}} \equiv \boldsymbol{H}\cdot\tilde{\boldsymbol{m}}. \tag{4.20}$$

The nonlinear MAP equation (4.19) can be represented conceptually by a block diagram, as shown in Fig. 2, but cannot be solved analytically in general. Although the block diagram seems to suggest that homodyne measurements of the quadrature $\boldsymbol{p}$ in a feedback system can be used to produce the estimated message $\tilde{\boldsymbol{m}}$, $\boldsymbol{p}$ depends recursively on $\tilde{\boldsymbol{\phi}}$, and the impulse response matrix $\boldsymbol{H}\cdot\boldsymbol{K}_m\cdot\boldsymbol{H}^T$ that transforms $\boldsymbol{p}$ to $\tilde{\boldsymbol{\phi}}$ is not necessarily causal. Even if one attempts to solve the MAP equation numerically, one needs the values of both quadratures of $\boldsymbol{a}$ at all times, so one would have to perform heterodyne detection and start with the Q distribution instead of the Wigner distribution.

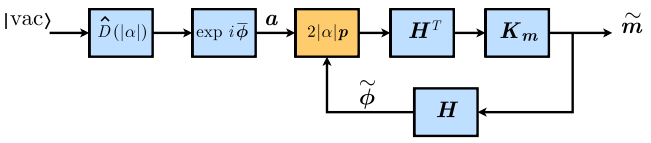

FIG. 2. (Color online). A block diagram that represents the MAP estimation process. $\hat{D}(|\alpha|)$ denotes displacement of the vacuum along the $\boldsymbol{x}_0$ quadrature, and $\exp i\bar{\boldsymbol{\phi}}$ denotes phase modulation.

To solve Eq. (4.19) approximately, let us linearize it so that the right-hand side of Eq. (4.19) depends linearly on $\tilde{\boldsymbol{m}}$ and we can use well-established linear estimation techniques to perform MAP estimation. Writing the complex field $\boldsymbol{a}$ in terms of $\boldsymbol{x}_0$ and $\boldsymbol{y}_0$ as

$$\boldsymbol{a} = \exp(i\bar{\boldsymbol{\phi}})\left(|\alpha| + \frac{\boldsymbol{x}_0 + i\boldsymbol{y}_0}{2}\right), \tag{4.21}$$

$\boldsymbol{p}$ can be rewritten as

$$\boldsymbol{p} = 2|\alpha|\sin(\bar{\boldsymbol{\phi}} - \tilde{\boldsymbol{\phi}}) + z_0, \tag{4.22}$$

where we have defined another quadrature field z_0 as

$$z_0 \equiv \boldsymbol{x}_0\sin(\bar{\boldsymbol{\phi}} - \tilde{\boldsymbol{\phi}}) + \boldsymbol{y}_0\cos(\bar{\boldsymbol{\phi}} - \tilde{\boldsymbol{\phi}}). \tag{4.23}$$

Quantum noise enters the MAP estimation through the z_0 quadrature. Because the vacuum Wigner distribution given by Eq. (4.15) is invariant with respect to rotations in phase space, any quadrature in terms of $\boldsymbol{x}_0$ and $\boldsymbol{y}_0$ has the same Gaussian statistics as $\boldsymbol{x}_0$ or $\boldsymbol{y}_0$ and its statistics are independent of $\bar{\boldsymbol{\phi}}$ or $\tilde{\boldsymbol{\phi}}$. z_0 can, therefore, be regarded as an independent noise term. To linearize $\boldsymbol{p}$, we assume that the estimated phase is at all times close to the mean phase of the field in the mean-square sense,

$$\langle(\bar{\boldsymbol{\phi}} - \tilde{\boldsymbol{\phi}})^2\rangle \ll \boldsymbol{1}, \tag{4.24}$$

so that we can make the first-order approximation

$$\boldsymbol{p} \approx 2|\alpha|(\bar{\boldsymbol{\phi}} - \tilde{\boldsymbol{\phi}}) + z_0. \tag{4.25}$$

A linearized MAP equation can thus be obtained,

$$\tilde{\boldsymbol{m}} \approx 4|\alpha|^2\boldsymbol{K}_m\cdot\boldsymbol{H}^T\cdot\left(\bar{\boldsymbol{\phi}} - \tilde{\boldsymbol{\phi}} + \frac{z_0}{2|\alpha|}\right). \tag{4.26}$$

In this linear regime, the MAP estimation is efficient. Let us define

$$\boldsymbol{\phi} \equiv \bar{\boldsymbol{\phi}} + \frac{z_0}{2|\alpha|}, \quad \boldsymbol{\epsilon} \equiv \boldsymbol{\phi} - \tilde{\boldsymbol{\phi}}, \tag{4.27}$$

so that the linearized MAP equation (4.26) can be written as a pair of equations,

$$\tilde{\boldsymbol{m}} = 4|\alpha|^2 \boldsymbol{K_m} \cdot \boldsymbol{H}^T \cdot \boldsymbol{\epsilon}, \tag{4.28}$$

$$\boldsymbol{\phi} - \boldsymbol{H} \cdot \tilde{\boldsymbol{m}} = \boldsymbol{\epsilon}. \tag{4.29}$$

Multiplying Eq. (4.28) by $\boldsymbol{H}$ and adding it to Eq. (4.29),

$$\boldsymbol{\phi} = (4|\alpha|^2 \boldsymbol{H} \cdot \boldsymbol{K_m} \cdot \boldsymbol{H}^T + \boldsymbol{I}) \cdot \boldsymbol{\epsilon}. \tag{4.30}$$

Comparing Eq. (4.30) with Eq. (4.28), we find that $\tilde{\boldsymbol{m}}$ can be written as a linear transformation of $\boldsymbol{\phi}$,

$$\tilde{\boldsymbol{m}} = \boldsymbol{G} \cdot \boldsymbol{\phi}, \tag{4.31}$$

where $\boldsymbol{G}$ is the solution of the following equation:

$$\boldsymbol{G} \cdot (4|\alpha|^2 \boldsymbol{H} \cdot \boldsymbol{K_m} \cdot \boldsymbol{H}^T + \boldsymbol{I}) = 4|\alpha|^2 \boldsymbol{K_m} \cdot \boldsymbol{H}^T. \tag{4.32}$$

To solve this equation, we assume that the message covariance matrix $\boldsymbol{K_m}$ is stationary, so that we can write

$$(\boldsymbol{K_m})_{jk} = K_{\boldsymbol{m},j-k}, \tag{4.33}$$

and define its power spectral density as

$$S_{\boldsymbol{m}}(f) \equiv \sum_j K_{\boldsymbol{m},j} \exp(i2\pi f t_j). \tag{4.34}$$

If $\boldsymbol{H}$ is time-invariant,

$$H_{jk} = H_{j-k}, \quad H(f) \equiv \sum_j H_j \exp(i2\pi f t_j), \tag{4.35}$$

we can solve Eq. (4.32) by Fourier transform and obtain a time-invariant solution for $\boldsymbol{G}$,

$$G(f) = \frac{4|\alpha|^2 S_{\boldsymbol{m}}(f) H^*(f)}{4|\alpha|^2 S_{\boldsymbol{m}}(f)|H(f)|^2 + 1}, \tag{4.36}$$

$$G_{j-k} = \frac{1}{B}\int_{-B/2}^{B/2} df G(f) \exp[-i2\pi f(t_j - t_k)]. \tag{4.37}$$

G_{j-k} is called the optimum filter in linear estimation theory [1,2]. In the next section, we shall show how the optimum filter can be implemented by a homodyne phase-locked loop.

B. Phase-locked loops as angle demodulators

Consider the homodyne phase-locked loop shown in Fig. 3. The output of the homodyne detection is given by

$$\boldsymbol{p}' = -i[\boldsymbol{a} \exp(-i\boldsymbol{\phi}') - \boldsymbol{a}^* \exp(i\boldsymbol{\phi}')] \tag{4.38}$$

$$= 2|\alpha| \sin(\bar{\boldsymbol{\phi}} - \boldsymbol{\phi}') + z', \tag{4.39}$$

where z' is another quadrature field defined as

$$z' \equiv \boldsymbol{x}_0 \sin(\bar{\boldsymbol{\phi}} - \boldsymbol{\phi}') + \boldsymbol{y}_0 \cos(\bar{\boldsymbol{\phi}} - \boldsymbol{\phi}'), \tag{4.40}$$

which, like z_0, has Gaussian statistics independent of $\bar{\boldsymbol{\phi}}$ and $\boldsymbol{\phi}'$. If we again linearize $\boldsymbol{p}'$ by making the assumption, to be justified later, that the local-oscillator phase $\boldsymbol{\phi}'$ is at all times close to the mean phase of the incoming field $\bar{\boldsymbol{\phi}}$,

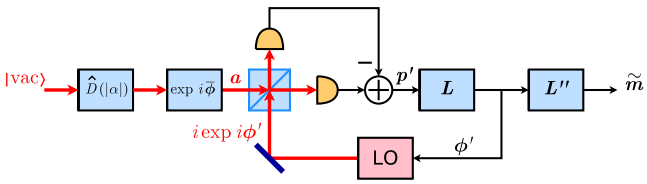

FIG. 3. (Color online) A homodyne phase-locked loop. LO denotes local oscillator.

$$\langle(\bar{\boldsymbol{\phi}} - \boldsymbol{\phi}')^2\rangle \ll \boldsymbol{1}, \tag{4.41}$$

$\boldsymbol{p}'$ is given by

$$\boldsymbol{p}' \approx 2|\alpha|(\boldsymbol{\phi} - \boldsymbol{\phi}'), \quad \boldsymbol{\phi} \equiv \bar{\boldsymbol{\phi}} + \frac{z'}{2|\alpha|}. \tag{4.42}$$

$\boldsymbol{\phi}'$ is related to $\boldsymbol{p}'$ by the causal loop filter $\boldsymbol{L}$,

$$\boldsymbol{\phi}' = \boldsymbol{L} \cdot \boldsymbol{p}' \approx \boldsymbol{L} \cdot 2|\alpha|(\boldsymbol{\phi} - \boldsymbol{\phi}'), \tag{4.43}$$

and $\boldsymbol{\phi}'$ can be written in terms of $\boldsymbol{\phi}$ and a closed-loop filter $\boldsymbol{L}'$,

$$\boldsymbol{\phi}' \approx \boldsymbol{L}' \cdot \boldsymbol{\phi}, \tag{4.44}$$

where the closed-loop filter satisfies the equation

$$(\boldsymbol{I} + 2|\alpha|\boldsymbol{L}) \cdot \boldsymbol{L}' = 2|\alpha|\boldsymbol{L}. \tag{4.45}$$

To minimize $\langle(\bar{\boldsymbol{\phi}} - \boldsymbol{\phi}')^2\rangle$ and ensure that Eq. (4.41) holds, we demand $\boldsymbol{\phi}'$ to be the minimum-mean-square-error estimate of $\bar{\boldsymbol{\phi}}$, using only past and present values of $\boldsymbol{p}'$ to ensure causality. For stationary $\boldsymbol{\phi}$, $\bar{\boldsymbol{\phi}}$, and z', $\boldsymbol{L}'$ is simply the Wiener filter and can be solved by a well-known frequency-domain technique [1,2], as briefly described below. L'_{j-k} is the solution of the discrete Wiener-Hopf equation,

$$\sum_{k=0}^{\infty} L'_k U_{j-k} = V_j, \tag{4.46}$$

$$\boldsymbol{U} \equiv 4|\alpha|^2 \boldsymbol{H} \cdot \boldsymbol{K_m} \cdot \boldsymbol{H}^T + \boldsymbol{I}, \tag{4.47}$$

$$\boldsymbol{V} \equiv 4|\alpha|^2 \boldsymbol{H} \cdot \boldsymbol{K_m} \cdot \boldsymbol{H}^T. \tag{4.48}$$

The Fourier transform of U_{j-k} can be factored into the form

$$U(f) = X(f)X^*(f), \tag{4.49}$$

where $X(f)$ and $1/X(f)$ are causal filters, if $U(f)$ is a rational spectral density. Defining

$$\left[\frac{V(f)}{X^*(f)}\right]_+ \equiv \frac{1}{B}\int_{-B/2}^{B/2} df' \frac{V(f')}{X^*(f')} \sum_{j=0}^{\infty} \exp[i2\pi(f - f')t_j], \tag{4.50}$$

the Fourier transform of L'_{j-k} is given by

$$L'(f) = \frac{1}{X(f)}\left[\frac{V(f)}{X^*(f)}\right]_+, \tag{4.51}$$

and the loop filter is then

$$L(f) = \frac{L'(f)}{2|\alpha|[1 - L'(f)]}. \tag{4.52}$$

It can be shown that the loop filter $\boldsymbol{L}$ is also causal given a causal $\boldsymbol{L}'$ [1,2]. After passing through the phase-locked loop and the post-loop filter $\boldsymbol{L}''$, the output estimated message becomes

$$\tilde{\boldsymbol{m}} \approx \boldsymbol{L}'' \cdot \boldsymbol{L}' \cdot \boldsymbol{\phi}. \tag{4.53}$$

This equation is the same as the linearized MAP equation (4.31) if

$$\boldsymbol{G} = \boldsymbol{L}'' \cdot \boldsymbol{L}'. \tag{4.54}$$

The post-loop filter in the frequency domain is thus given by

$$L''(f) = \frac{G(f)}{L'(f)}. \tag{4.55}$$

To make the post-loop filter realizable, we allow delay in the estimated message, that is, we let

$$\bar{\phi}_j = \sum_k H_{j-k} m_{k+d}, \quad \tilde{\phi}_j = \sum_k H_{j-k} \tilde{m}_{k+d}, \tag{4.56}$$

and $\boldsymbol{L}''$ can be made causal in the limit of infinite delay d [1,2]. In practice, $d\delta t$ only needs to be a few times larger than the correlation time of the message for $\boldsymbol{L}''$ to be well approximated by causal filters. Hence, the homodyne phase-locked loop is able to realize the MAP estimation for coherent states, provided that the approximation given by Eq. (4.41) is valid and the local-oscillator phase follows closely the mean phase of the incoming field at all times. This result is hardly surprising, because a coherent state can be regarded as a classical signal with additive white Gaussian noise, in which case it is well known that the homodyne phase-locked loop realizes the optimum angle demodulator [1,2]. Our analysis so far closely mirrors that in classical estimation theory, except that we have worked with discrete time for consistency with previous sections. It is straightforward to take the continuous limit of our analysis in this section, if one so desires, by redefining some of the quantities and taking the limit $B \to \infty$.

C. Squeezed states

The MAP estimation analysis shows that quantum noise enters the estimation through the z_0 quadrature, which depends on both $\boldsymbol{x}_0$ and $\boldsymbol{y}_0$. If we squeeze the z_0 quadrature of the vacuum before displacement and phase modulation, the noise entering the measurement of $\boldsymbol{p}$ can be reduced. The squeezed-vacuum Wigner distribution is

$$W_0[\boldsymbol{x}_0, \boldsymbol{y}_0] \propto \exp\left(-\frac{1}{2}\boldsymbol{\zeta}_0 \cdot \boldsymbol{K}_1^{-1} \cdot \boldsymbol{\zeta}_0 - \frac{1}{2} z_0 \cdot \boldsymbol{K}_2^{-1} \cdot z_0\right), \tag{4.57}$$

$$\boldsymbol{\zeta}_0 = \boldsymbol{x}_0 \cos(\bar{\boldsymbol{\phi}} - \tilde{\boldsymbol{\phi}}) - \boldsymbol{y}_0 \sin(\bar{\boldsymbol{\phi}} - \tilde{\boldsymbol{\phi}}), \tag{4.58}$$

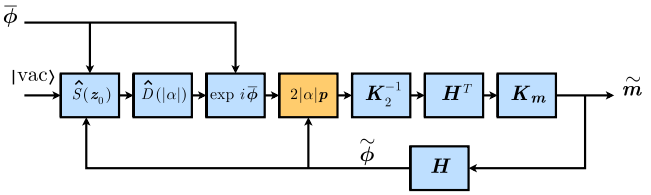

FIG. 4. (Color online) MAP estimation for squeezed states. $\hat{S}(z_0)$ denotes squeezing of the z_0 quadrature.

$$z_0 = \boldsymbol{x}_0 \sin(\bar{\boldsymbol{\phi}} - \tilde{\boldsymbol{\phi}}) + \boldsymbol{y}_0 \cos(\bar{\boldsymbol{\phi}} - \tilde{\boldsymbol{\phi}}), \tag{4.59}$$

$$\boldsymbol{K}_1 \equiv \langle \boldsymbol{\zeta}_0 \otimes \boldsymbol{\zeta}_0 \rangle, \quad \boldsymbol{K}_2 \equiv \langle z_0 \otimes z_0 \rangle. \tag{4.60}$$

The MAP equation becomes

$$\tilde{\boldsymbol{m}} = 2|\alpha| \boldsymbol{K}_m \cdot \boldsymbol{H}^T \cdot \boldsymbol{K}_2^{-1} \cdot \boldsymbol{p}, \tag{4.61}$$

as shown schematically in Fig. 4. The linearized MAP equation is the same as Eq. (4.31), but $\boldsymbol{G}$ now also depends on $\boldsymbol{K}_2$,

$$\boldsymbol{G} \cdot (4|\alpha|^2 \boldsymbol{H} \cdot \boldsymbol{K}_m \cdot \boldsymbol{H}^T + \boldsymbol{K}_2) = 4|\alpha|^2 \boldsymbol{K}_m \cdot \boldsymbol{H}^T. \tag{4.62}$$

A homodyne phase-locked loop, with redesigned loop and post-loop filters $\boldsymbol{L}$ and $\boldsymbol{L}''$ according to the $\boldsymbol{G}$ given by Eq. (4.62), can again be used to realize this MAP estimation, as shown in Fig. 5, although one must feed the local-oscillator phase $\boldsymbol{\phi}'$ back to the quantum-state preparation stage in order to squeeze the right quadrature of the vacuum. The time delay of the feedback path must be much shorter than the time scale at which the phase modulation varies.

If the feedback of $\boldsymbol{\phi}'$ and the z'-quadrature squeezing is not feasible in practice, another option is to use an ideal phase-squeezed state and squeeze the $\boldsymbol{y}_0$ quadrature of the vacuum before displacement and phase modulation. The squeezed-vacuum Wigner distribution is

$$W_0[\boldsymbol{x}_0, \boldsymbol{y}_0] \propto \exp\left(-\frac{1}{2}\boldsymbol{x}_0 \cdot \boldsymbol{K}_1^{-1} \cdot \boldsymbol{x}_0 - \frac{1}{2}\boldsymbol{y}_0 \cdot \boldsymbol{K}_2^{-1} \cdot \boldsymbol{y}_0\right). \tag{4.63}$$

The MAP equation becomes

$$\tilde{\boldsymbol{m}} = \boldsymbol{K}_m \cdot \boldsymbol{H}^T \cdot \boldsymbol{\eta}, \tag{4.64}$$

where

$$\boldsymbol{\eta} \equiv \boldsymbol{q}(\boldsymbol{K}_2^{-1} \cdot \boldsymbol{p}) + \boldsymbol{p}[\boldsymbol{K}_1^{-1} \cdot (2|\alpha| - \boldsymbol{q})], \tag{4.65}$$

$$\boldsymbol{q} \equiv \boldsymbol{a} \exp(-i\tilde{\boldsymbol{\phi}}) + \boldsymbol{a}^* \exp(i\tilde{\boldsymbol{\phi}}), \tag{4.66}$$

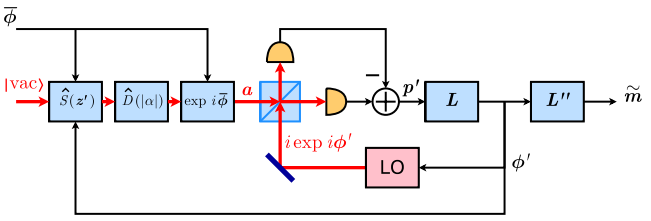

FIG. 5. (Color online) A homodyne phase-locked loop that realizes the MAP estimation for squeezed states. $\hat{S}(z')$ denotes squeezing of the z' quadrature.

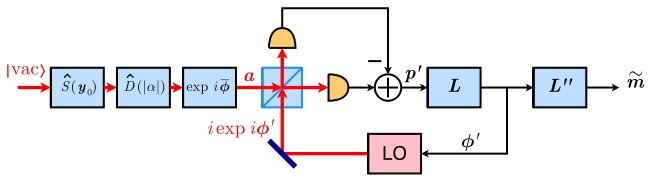

FIG. 6. (Color online) A homodyne phase-locked loop for phase-squeezed states.

$$p \equiv -i[a\exp(-i\tilde{\phi}) - a^*\exp(i\tilde{\phi})]. \tag{4.67}$$

The MAP equation now depends quadratically on two quadrature fields q and p. Realizing this MAP estimation would require some nontrivial second-order field measurements of η in a Weyl-ordered operator form for the statistics to obey the Wigner distribution.

If we insist on using the homodyne phase-locked loop for phase-squeezed states, the noise term of the homodyne detection z' in the first order of small $\langle(\bar{\phi}-\phi')^2\rangle$ is given by

$$z' \approx x_0(\bar{\phi}-\phi') + y_0. \tag{4.68}$$

The y_0 quadrature is squeezed, but the antisqueezed x_0 quadrature also enters the phase-locked loop through the phase-sensitive term $x_0(\bar{\phi}-\phi')$, the magnitude of which varies depending on the difference between the mean phase and the local-oscillator phase. If the magnitude of $x_0(\bar{\phi}-\phi')$ is much smaller than the magnitude of y_0, however, we can assume that z' is approximately y_0,

$$z' \approx y_0, \tag{4.69}$$

and the homodyne phase-locked loop can still be used, as shown in Fig. 6, with the same filters as those designed for the G given by Eq. (4.62).

Because z' passes through the loop filter L before entering the system, the approximation $z' \approx y_0$ requires

$$\langle(\bar{\phi}-\phi')^2\rangle \ll \frac{\langle(L\cdot y_0)^2\rangle}{\langle(L\cdot x_0)^2\rangle}. \tag{4.70}$$

If the constraint given by Eq. (4.70) is violated, z' cannot be regarded as a phase-insensitive noise term, and the phase-locked loop is no longer an accurate realization of MAP estimation for phase-squeezed states. It might still be possible to heuristically adjust the parameters of the phase-locked loop to compensate for the phase-sensitive noise and minimize the estimation error, but Eq. (4.70) sets a rough limit on the right amount of squeezing, beyond which stronger squeezing is no longer useful.

If one is able to perform canonical temporal-phase measurements, then the homodyne detection in the phase-locked loop shown in Fig. 6 can be replaced with measurements of $\sin(\phi-\phi')$, where ϕ is the canonical phase of the incoming field a. Canonical phase measurements are not sensitive to the antisqueezed photon-number noise, so the squeezing constraint given by Eq. (4.70) is not needed, although the constraint given by Eq. (4.41) is still required for the estimation to remain efficient in the linear regime.

The adaptive temporal-phase measurement scheme proposed by Berry and Wiseman [29] is essentially a first-order homodyne phase-locked loop, with an integrator as the loop filter and no post-loop filter. While the first-order phase-locked loop is indeed the optimal demodulator when the mean phase is a Wiener random process [2], it is clear from the preceding discussion that, at least for stationary messages, one should use a more complicated loop filter as well as a post-loop filter according to the *a priori* message statistics to minimize the estimation error. In this paper, we focus on stationary messages and the use of MAP estimation to design angle demodulators. For nonstationary messages, it is more appropriate to use a state-variable approach and Kalman-Bucy filters [2,38], although it is beyond the scope of this paper to study the latter case.

V. QUANTUM LIMITS TO ANGLE DEMODULATION

To calculate the mean-square error in the estimated message by MAP estimation, consider the linearized MAP equation

$$\tilde{m} = G\cdot\phi = G\cdot H\cdot m + G\cdot\frac{z'}{2|\alpha|}. \tag{5.1}$$

The mean-square error is

$$\langle(\tilde{m}-m)^2\rangle \approx \mathrm{diag}\left\{(G\cdot H - I)\cdot K_m\cdot(G\cdot H - I)^T + \frac{1}{4|\alpha|^2}G\cdot K_2\cdot G^T\right\}, \tag{5.2}$$

where $\mathrm{diag}(A)_j = A_{jj}$ is the diagonal vector component of A. Equation (5.2) can be further simplified in the Fourier domain to give

$$\sigma^2 \equiv \langle(\tilde{m}_j - m_j)^2\rangle \approx \frac{1}{B}\int_{-B/2}^{B/2} df \frac{S_m(f)S_2(f)}{4|\alpha|^2 S_m(f)|H(f)|^2 + S_2(f)}, \tag{5.3}$$

where $S_2(f)$ is the power spectral density of the z' quadrature. This expression is well known in linear estimation theory and called the irreducible error [1,2]. Assuming that the message has unit variance $\langle m_j^2\rangle = 1$ and a flat spectral density with bandwidth b,

$$S_m(f) = \begin{cases} B/b, & |f| < b/2, \\ 0, & |f| \geq b/2. \end{cases} \tag{5.4}$$

If $S_2(f)$ is also flat over the bandwidth b, the mean-square error for PM becomes

$$\sigma^2_{\mathrm{PM}} = \frac{1}{\beta^2\Lambda + 1} \approx \frac{1}{\beta^2\Lambda}, \quad \beta^2\Lambda \gg 1, \tag{5.5}$$

where we have defined the parameter Λ as

$$\Lambda \equiv \frac{4|\alpha|^2 S_m(0)}{S_2(0)}. \tag{5.6}$$

The SNR is then

$$(\mathrm{SNR}_{\mathrm{PM}}) \equiv \frac{\langle m_I^2 \rangle}{\sigma_{\mathrm{PM}}^2} \approx \beta^2 \Lambda. \tag{5.7}$$

For FM, defining the equivalent modulation index as

$$\beta \equiv \frac{2\mathcal{F}}{b}, \tag{5.8}$$

the mean-square error is

$$\sigma_{\mathrm{FM}}^2 = 1 - \sqrt{\beta^2 \Lambda} \tan^{-1} \frac{1}{\sqrt{\beta^2 \Lambda}} \approx \frac{1}{3\beta^2 \Lambda}, \quad \beta^2 \Lambda \gg 1, \tag{5.9}$$

and the SNR is

$$(\mathrm{SNR}_{\mathrm{FM}}) \approx 3\beta^2 \Lambda. \tag{5.10}$$

The parameter Λ depends on the ratio of the message spectral density to the quadrature-noise spectral density.

A. Standard and Heisenberg quantum limits

For a coherent state with average optical power

$$\mathcal{P} \equiv h f_0 B \langle \hat{a}^\dagger \hat{a} \rangle = h f_0 B |\alpha|^2 \tag{5.11}$$

and a quadrature-noise spectral density

$$S_2(f) = 1, \tag{5.12}$$

Λ is

$$\Lambda = \frac{4\mathcal{P}}{h f_0 b} \equiv 4\mathcal{N}, \quad \mathcal{N} \equiv \frac{\mathcal{P}}{h f_0 b}, \tag{5.13}$$

where $\mathcal{N}$ is the average number of photons in a period of $1/b$, and the $\sigma^2 \sim 1/\mathcal{N}$ dependence is an analog of the usual standard quantum limit (SQL) in single-parameter estimation [10]. We can then write the SNR at SQL as

$$(\mathrm{SNR}_{\mathrm{PM}}) \approx \frac{1}{3}(\mathrm{SNR}_{\mathrm{FM}}) \approx 4\beta^2 \mathcal{N} \quad (\mathrm{SQL}). \tag{5.14}$$

This linear dependence on $\mathcal{N}$ may not hold for non-band-limited message spectral densities. For example, if we let the message spectral density be Lorentzian,

$$S_{\boldsymbol{m}}(f) = \frac{B}{2\pi} \frac{b}{f^2 + (b/2)^2}, \tag{5.15}$$

the PM SNR for a coherent state in the limit of $B \gg b$ is

$$(\mathrm{SNR}_{\mathrm{PM}}) \approx \sqrt{\frac{8\beta^2 \mathcal{N}}{\pi} + 1}, \tag{5.16}$$

which scales with $\sqrt{\mathcal{N}}$ instead of $\mathcal{N}$. A similar $\sqrt{\mathcal{N}}$ scaling is also observed by Berry and Wiseman for their adaptive temporal-phase measurement scheme with the nonstationary Wiener process as the mean phase [29]. In the following, we consider only the band-limited message spectral density given by Eq. (5.4) for simplicity.

For squeezed states, it is shown in Appendix B that

$$S_2(f) = \exp(-2r) \quad \text{for } |f| < \frac{B_s}{2}, \tag{5.17}$$

where r is the squeeze parameter and B_s is the squeeze bandwidth. We should therefore make B_s at least as large as the message bandwidth b. The average power of a squeezed state is

$$\mathcal{P} = h f_0 B |\alpha|^2 + h f_0 B_s \sinh^2 r. \tag{5.18}$$

Assuming $B_s = b$,

$$\Lambda = 4(\mathcal{N} - \sinh^2 r)\exp(2r), \tag{5.19}$$

the SNRs become

$$(\mathrm{SNR}_{\mathrm{PM}}) \approx \frac{1}{3}(\mathrm{SNR}_{\mathrm{FM}}) \approx 4\beta^2(\mathcal{N} - \sinh^2 r)\exp(2r). \tag{5.20}$$

The optimal $\exp(2r)$ at which the SNRs in Eq. (5.20) are maximum is given by

$$\exp(2r) = 2\mathcal{N} + 1, \tag{5.21}$$

and the maximum SNRs become

$$(\mathrm{SNR}_{\mathrm{PM}}) \approx \frac{1}{3}(\mathrm{SNR}_{\mathrm{FM}}) \approx 4\beta^2 \mathcal{N}(\mathcal{N} + 1) \quad (\mathrm{Heisenberg}). \tag{5.22}$$

The $\mathcal{N}^2$ scaling can be regarded as an analog of the Heisenberg limit in quantum single-parameter estimation [10].

B. Threshold constraint

It must be stressed that the preceding derivation of quantum limits is accurate only in the linear regime, when the constraint given by Eq. (4.41) is satisfied. Beyond the linear regime, the phase-locked-loop demodulator is no longer an efficient estimator, and the SNR is expected to drop abruptly when the quantum noise is larger than a certain threshold. Physically, the abrupt drop in SNR below threshold is due to the periodic nature of $\boldsymbol{p}'$ with respect to $\bar{\boldsymbol{\phi}} - \boldsymbol{\phi}'$, which can cause $\boldsymbol{\phi}'$ to differ from $\bar{\boldsymbol{\phi}}$ by multiples of 2π when the noise is large. To ensure that the estimation is efficient, Eq. (4.41), which we now call the threshold constraint in accordance with classical theory, should be observed. Since we have assumed that the z'-quadrature spectral density is flat over the message bandwidth, an expression for $\langle (\bar{\phi}_j - \phi_j')^2 \rangle$ can be borrowed from well known results for classical signals with additive white Gaussian noise [1,2]. For the flat message spectral density,

$$\sigma_0^2 \equiv \langle (\bar{\phi}_j - \phi_j')^2 \rangle \approx \frac{1}{b\Lambda} \int_{-b/2}^{b/2} df \ln[1 + \Lambda |H(f)|^2]. \tag{5.23}$$

The threshold constraint for PM becomes

$$\frac{1}{\Lambda}\ln(1+\beta^2\Lambda) \ll 1, \tag{5.24}$$

while the constraint for FM is

$$\frac{1}{\Lambda}\left[\ln(1+\beta^2\Lambda) + 2\beta\sqrt{\Lambda}\tan^{-1}\left(\frac{1}{\beta\sqrt{\Lambda}}\right)\right] \ll 1. \tag{5.25}$$

In practice, it has been determined numerically for classical signals with additive white Gaussian noise that $\sigma_0^2 \leqslant 0.25$ is sufficient to satisfy the threshold constraint [1,2], so a similar constraint on σ_0^2 can be used for coherent states or z'-quadrature-squeezed states.

C. Squeezing constraint

For phase-squeezed states and the homodyne phase-locked loop depicted in Fig. 6, one should also apply the squeezing constraint (4.70) for the SNR to be given by Eq. (5.20). The order of magnitude of the right-hand side of Eq. (4.70) is calculated in Appendix B and is roughly $\exp(-4r)$. The constraint becomes

$$\frac{\exp(4r)}{\Lambda}\ln(1+\beta^2\Lambda) \ll 1 \tag{5.26}$$

for PM and

$$\frac{\exp(4r)}{\Lambda}\left[\ln(1+\beta^2\Lambda) + 2\beta\sqrt{\Lambda}\tan^{-1}\left(\frac{1}{\beta\sqrt{\Lambda}}\right)\right] \ll 1 \tag{5.27}$$

for FM, where Λ is given by Eq. (5.19). The squeezing constraint is much more stringent than the threshold constraint and more so for stronger squeezing, because the former constraint requires the enhanced noise in the antisqueezed $\boldsymbol{x}_0$ quadrature to be negligible.

The squeezing constraint also prevents the homodyne phase-locked loop with phase-squeezed states from reaching the Heisenberg limit given by Eq. (5.22). Consider, for example, the left-hand side of Eq. (5.26) at the Heisenberg limit,

$$\frac{(2\mathcal{N}+1)^2}{4\mathcal{N}(\mathcal{N}+1)}\ln(1+4\beta^2\mathcal{N}^2), \tag{5.28}$$

which is much smaller than 1 only when $4\beta^2\mathcal{N}^2 \ll 1$ and the exact SNR approaches its lowest possible value 1, the *a priori* SNR. If we let $\exp(2r)$ be a small parameter λ times $\mathcal{N}$ instead,

$$\exp(2r) = \lambda\mathcal{N}, \quad \lambda \ll 1, \quad \Lambda \approx 4\lambda\mathcal{N}^2, \tag{5.29}$$

Eq. (5.26) becomes

$$\lambda \ll \frac{4}{\ln(1+4\lambda\beta^2\mathcal{N}^2)} \approx \frac{2}{\ln\mathcal{N}} \tag{5.30}$$

for $4\delta\beta^2\mathcal{N}^2 \gg 1$ and $\ln\mathcal{N} \gg \ln(2\sqrt{\lambda}\beta)$. The SNR for PM is therefore limited by

$$(\mathrm{SNR}_{\mathrm{PM}}) \approx 4\lambda\beta^2\mathcal{N}^2 \ll \frac{8\beta^2\mathcal{N}^2}{\ln\mathcal{N}} \tag{5.31}$$

in the limit of large $\mathcal{N}$. The limit on the FM SNR can be derived using a similar argument, and is given by

$$(\mathrm{SNR}_{\mathrm{FM}}) \ll \frac{24\beta^2\mathcal{N}^2}{\ln\mathcal{N}} \tag{5.32}$$

in the limit of large $\mathcal{N}$. The $\mathcal{N}^2/\ln\mathcal{N}$ scaling is analogous to the ultimate limit to adaptive single-mode phase measurements [28].

D. SNR enhancement by wideband angle modulation

Apart from the quantum enhancement by squeezing, the SNRs above threshold can be enhanced quadratically for a band-limited message spectral density simply by increasing the modulation index β. This SNR enhancement is achieved at the expense of bandwidth resource, as is well known in classical communication [1–3]. The SNR enhancement effect for discrete FM in the quantum regime has also been suggested by Yuen [7]. A good approximation of the optical signal bandwidth B when the phase or instantaneous frequency of a monochromatic wave is modulated by a message with unit variance $\langle m_j^2\rangle = 1$, bandwidth b, and modulation index β is provided by Carson's rule [3],

$$B \approx (\beta+1)b. \tag{5.33}$$

The modulation is described as narrowband when $\beta \ll 1$, wideband when $\beta \sim 1$, and ultrawideband when $\beta \gg 1$. For squeezed states, because they already have an inherent bandwidth B_s before phase modulation, Carson's rule should be modified to read

$$B \approx B_s + (\beta+1)b. \tag{5.34}$$

For a given Λ, β is also limited by the threshold constraint given by Eqs. (5.24)–(5.26), or (5.27), since σ_0^2 increases logarithmically with β. Thus β cannot be increased indefinitely even if enough optical bandwidth is available.

VI. OPTICAL SENSING OF POSITION AND VELOCITY

The preceding analysis can be applied directly to optical sensing of position and velocity, if the phase modulation is due to reflection off a classical moving target. Consider the setup shown in Fig. 7. A light beam, which can be a coherent state or squeezed states, shines on a reflecting target and bounces back and forth between the target and a perfectly reflecting mirror for M times before leaving the apparatus. The phase modulation due to the movement of the target is then estimated using canonical temporal-phase measurements or a phase-locked loop. The mean phase of the output light beam is given by

$$\bar{\phi}(t) = (2M\cos\theta)\frac{2\pi}{\lambda_0}x(t) \tag{6.1}$$

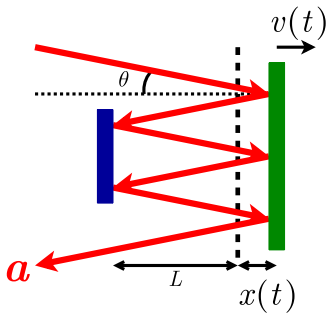

FIG. 7. (Color online) Multipass position and velocity sensor.

$$= (2M\cos\theta)\frac{2\pi f_0}{c}\int_{-\infty}^{t} dt' v(t'). \quad (6.2)$$

The quantum limits derived in the preceding section are also applicable here, if we assume that the target position and velocity are stationary random processes and define the normalized PM and FM parameters in terms of the sensing parameters as

$$\beta = 2M\cos\theta\frac{2\pi\sqrt{\langle x^2(t)\rangle}}{\lambda_0}, \quad (6.3)$$

$$m(t) = \frac{x(t)}{\sqrt{\langle x^2(t)\rangle}} \quad (6.4)$$

for position sensing, and

$$\mathcal{F} = (2M\cos\theta)\frac{f_0\sqrt{\langle v^2(t)\rangle}}{c}, \quad (6.5)$$

$$\beta = (2M\cos\theta)\frac{2f_0\sqrt{\langle v^2(t)\rangle}}{bc}, \quad (6.6)$$

$$m(t) = -\frac{v(t)}{\sqrt{\langle v^2(t)\rangle}} \quad (6.7)$$

for velocity sensing. The power spectral densities of the position and velocity are related to each other by

$$S_x(f) = \frac{1}{(2\pi f)^2}S_v(f), \quad (6.8)$$

so one should calculate the mean-square errors for position and velocity estimations separately using Eq. (5.3). It is apparent from Eq. (5.3) that increasing β and therefore $H(f)$ can at best reduce the mean-square errors of the estimations quadratically. Even though the parameters $\langle x^2(t)\rangle$, $\langle v^2(t)\rangle$, and b are given for each target, it is still possible to enhance the SNR by increasing M, the number of times the target is interrogated. In practice the maximum achievable M is limited by the threshold constraint as well as other experimental constraints. For instance, the total interrogation time of the light beam with the target should be much shorter than the time scale at which the position and the velocity changes, or in other words,

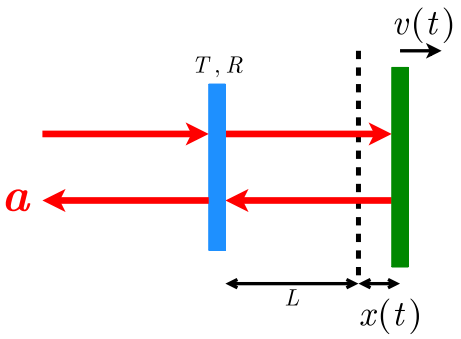

FIG. 8. (Color online) Fabry-Pérot position and velocity sensor.

$$\frac{2(M-1)L}{c\cos\theta} \ll \frac{1}{b}. \quad (6.9)$$

The target size, shape, and reflectivity also limit the maximum achievable M in practice.

The multipass setup may be regarded as a continuous-parameter generalization of multipass single-parameter quantum estimation schemes [10,11]. For single-parameter estimation, the multipass SNR enhancement is achieved at the expense of time, whereas for continuous-parameter estimation the enhancement effect utilizes both time and bandwidth resources. Squeezing becomes useful when such resources are limited, and the experiment can be highly controlled to eliminate decoherence, such as that caused by the imperfect reflectivity of the target or other optical losses in the system.

To achieve a large effective M, one may also use a Fabry-Pérot setup, as shown in Fig. 8, similar to the interferometric gravitational wave detector with Fabry-Pérot arms [39]. $\cos\theta$ becomes 1, and the effective M at resonance is

$$M = \frac{1+\sqrt{R}}{1-\sqrt{R}}. \quad (6.10)$$

Because the resonance condition is sensitive to the phase shift by the target, the Fabry-Pérot configuration is useful only in the narrowband modulation regime $\beta \ll 1$. Apart from this restriction, the preceding discussion on the multipass configuration applies to the Fabry-Pérot setup as well.

VII. FLUID VELOCITY OPERATOR FOR NONRELATIVISTIC BOSONS

We now apply the time-domain optical formalism described in Secs. II and III to nonrelativistic bosons in three spatial dimensions. In momentum space, the boson annihilation and creation operators obey the commutation relation

$$[\hat{a}(\mathbf{k}), \hat{a}^\dagger(\mathbf{k}')] = \delta^3(\mathbf{k}-\mathbf{k}'). \quad (7.1)$$

If we regard the nonrelativistic theory as an effective theory that ceases to be accurate beyond a certain range of momenta, we can explicitly impose a momentum cutoff to the Hilbert space, analogous to the bandwidth limitation on optical fields in Sec. II,

$$|k_x|,|k_y|,|k_z| < K, \tag{7.2}$$

so that we can discretize space as

$$\mathbf{x}_\mathbf{j} \equiv \mathbf{x}_0 + \mathbf{j}\,\delta x, \quad \mathbf{j} \equiv j\mathbf{e}_x + k\mathbf{e}_y + l\mathbf{e}_z, \quad \delta x \equiv \frac{\pi}{K}. \tag{7.3}$$

We can then define the space-domain operator as

$$\hat{A}(\mathbf{x}) = \frac{1}{(2\pi)^{3/2}} \int_{-K}^{K} dk_x \int_{-K}^{K} dk_y \int_{-K}^{K} dk_z \hat{a}(\mathbf{k}) \exp(i\mathbf{k}\cdot\mathbf{x}), \tag{7.4}$$

and the discrete wave-packet-mode annihilation operator as

$$\hat{a}_\mathbf{j} \equiv \hat{A}(\mathbf{x}_\mathbf{j})(\delta x)^{3/2}, \tag{7.5}$$

with the commutator

$$[\hat{a}_\mathbf{j}, \hat{a}^\dagger_{\mathbf{j}'}] = \delta_{\mathbf{j}\mathbf{j}'}. \tag{7.6}$$

The Hilbert space can be spanned by Fock states,

$$|n_\mathbf{j}\rangle_\mathbf{j} \equiv \sum_{n_\mathbf{j}=0}^{\infty} \frac{(\hat{a}^\dagger_\mathbf{j})^{n_\mathbf{j}}}{\sqrt{n_\mathbf{j}!}} |0\rangle_\mathbf{j}, \quad |\boldsymbol{n}\rangle \equiv \bigotimes_\mathbf{j} |n_\mathbf{j}\rangle_\mathbf{j}. \tag{7.7}$$

Unlike photons, the total number of massive bosons is conserved and usually fixed, so it is physically justifiable to impose upper limits to the boson numbers, so that the Hilbert space consists only of finite-boson-number states,

$$\hat{\mathbf{1}} = \sum_{\boldsymbol{n}=0}^{\boldsymbol{s}} |\boldsymbol{n}\rangle\langle\boldsymbol{n}|, \tag{7.8}$$

where $\boldsymbol{s} = \{\ldots, s_\mathbf{j}, \ldots\}$ and for simplicity we let $s_\mathbf{j}$ be the total number of bosons N.

With the finite-momentum and finite-boson-number Hilbert space, we can now apply the Pegg-Barnett theory [16] and define the unitary exponential-phase operator as

$$\exp(i\hat{\phi}_\mathbf{j}) \equiv \sum_{n_\mathbf{j}=0}^{N} |n_\mathbf{j} - 1\rangle_\mathbf{j}\langle n_\mathbf{j}| + \exp[i(N+1)\phi_{0\mathbf{j}}]|N\rangle_\mathbf{j}\langle 0|. \tag{7.9}$$

Most importantly, the action of this operator on the vacuum state is uniquely defined as

$$\exp(i\hat{\phi}_\mathbf{j})|0\rangle_\mathbf{j} = \exp[i(N+1)\phi_{0\mathbf{j}}]|N\rangle_\mathbf{j}, \tag{7.10}$$

which makes the operator unitary and distinguishes it from the nonunitary Susskind-Glogower operator.

The creation and annihilation operators can be rewritten as

$$\hat{a}_\mathbf{j} = \exp(i\hat{\phi}_\mathbf{j})\sqrt{\hat{n}_\mathbf{j}}, \quad \hat{a}^\dagger_\mathbf{j} = \sqrt{\hat{n}_\mathbf{j}}\exp(-i\hat{\phi}_\mathbf{j}). \tag{7.11}$$

Since the Hamiltonian is a function of $\hat{a}_\mathbf{j}$ and $\hat{a}^\dagger_\mathbf{j}$, the unphysical jump from the vacuum state to the maximum-number state indicated by Eq. (7.10) due to the action of the Pegg-Barnett operator cannot occur directly in the dynamics.

The commutation relation between the Pegg-Barnett operator and the number operator $\hat{n}_\mathbf{j} \equiv \hat{a}^\dagger_\mathbf{j}\hat{a}_\mathbf{j}$ is

$$[\exp(i\hat{\phi}_\mathbf{j}), \hat{n}_\mathbf{j}] = [1 - (N+1)|N\rangle_\mathbf{j}\langle N|]\exp(i\hat{\phi}_\mathbf{j}). \tag{7.12}$$

To define a fluid velocity operator, consider the semiclassical definition of a superfluid velocity field [23],

$$\mathbf{v}(\mathbf{x}) \equiv \frac{\hbar}{m}\nabla_\mathbf{x}\phi(\mathbf{x}), \tag{7.13}$$

where m is the mass of each boson. Because $\varphi(\mathbf{x})$ can be a multivalued function and is undefined where the fluid density is zero, Eq. (7.13) is ill-defined even in the semiclassical regime. An alternative is to consult the definition of the current density [25,26],

$$\mathbf{J}(\mathbf{x}) \equiv \frac{\hbar}{2im}[A^*(\mathbf{x})\nabla_\mathbf{x}A(\mathbf{x}) - A(\mathbf{x})\nabla_\mathbf{x}A^*(\mathbf{x})] \tag{7.14}$$

and define the analogous fluid velocity in terms of the exponential-phase function,

$$\mathbf{v}(\mathbf{x}) \equiv \frac{\hbar}{2im}\{\exp[-i\phi(\mathbf{x})]\nabla_\mathbf{x}\exp[i\phi(\mathbf{x})] - \exp[i\phi(\mathbf{x})]\nabla_\mathbf{x}\exp[-i\phi(\mathbf{x})]\} \tag{7.15}$$

$$= \frac{\hbar}{m}\nabla_{\mathbf{x}'}\sin[\phi(\mathbf{x}') - \phi(\mathbf{x})]|_{\mathbf{x}'=\mathbf{x}}, \tag{7.16}$$

which is equivalent to Eq. (7.13), where $\varphi(\mathbf{x})$ is continuous, and the sine function is always single-valued where $\varphi(\mathbf{x})$ is defined. But we have not yet solved the problem of defining $\varphi(\mathbf{x})$ where the density is zero. This can be done by regarding $\varphi(\mathbf{x})$ as a random function, or in the quantum regime, an operator. In the discrete space domain, we can define the fluid velocity operator as

$$\hat{\mathbf{v}}_\mathbf{j} \equiv \sum_{\mathbf{j}'} \mathbf{D}_{\mathbf{j}-\mathbf{j}'}\sin(\hat{\phi}_{\mathbf{j}'} - \hat{\phi}_\mathbf{j}), \tag{7.17}$$

where

$$\sin(\hat{\phi}_{\mathbf{j}'} - \hat{\phi}_\mathbf{j}) \equiv \frac{1}{2i}[\exp(i\hat{\phi}_{\mathbf{j}'} - i\hat{\phi}_\mathbf{j}) - \text{H.c.}]. \tag{7.18}$$

$\mathbf{D}_{\mathbf{j}-\mathbf{j}'}$ is the discrete impulse response that corresponds to the gradient operator,

$$\mathbf{D}_{\mathbf{j}-\mathbf{j}'} \equiv \frac{1}{\delta x}(d_{j-j'}\delta_{kk'}\delta_{ll'}\mathbf{e}_x + d_{k-k'}\delta_{jj'}\delta_{ll'}\mathbf{e}_y + d_{l-l'}\delta_{jj'}\delta_{kk'}\mathbf{e}_z), \tag{7.19}$$

where $d_{j-j'}$ is the differentiator given by Eq. (3.13). Neglecting the $|N\rangle_\mathbf{j}\langle N|$ term in the commutator in Eq. (7.12), which is important only in the highly unlikely event that all bosons are in the same spatial wave-packet mode, we arrive at the following velocity-number commutation relation:

$$[\hat{v}_\mathbf{j}, \hat{n}_{\mathbf{j}'}] \approx -i\frac{\hbar}{m}\mathbf{D}_{\mathbf{j}-\mathbf{j}'}\cos(\hat{\phi}_{\mathbf{j}'} - \hat{\phi}_\mathbf{j}). \tag{7.20}$$

In the limit of $\delta x \to 0$,

$$\hat{\mathbf{v}}_\mathbf{j} \to \hat{\mathbf{v}}(\mathbf{x}), \tag{7.21}$$

$$\hat{n}_{\mathbf{j}} \to \delta x^3 \hat{\rho}(\mathbf{x}), \tag{7.22}$$

$$\mathbf{D}_{\mathbf{j}-\mathbf{j}'} \to \delta x^3 \nabla_{\mathbf{x}} \delta^3(\mathbf{x}-\mathbf{x}'), \tag{7.23}$$

$$\cos(\hat{\phi}_{\mathbf{j}'} - \hat{\phi}_{\mathbf{j}}) \to \cos[\hat{\phi}(\mathbf{x}') - \hat{\phi}(\mathbf{x})], \tag{7.24}$$

we have

$$[\hat{\mathbf{v}}(\mathbf{x}), \hat{\rho}(\mathbf{x}')] \approx -i\frac{\hbar}{m}\nabla_{\mathbf{x}}\delta^3(\mathbf{x}-\mathbf{x}')\cos[\hat{\phi}(\mathbf{x}') - \hat{\phi}(\mathbf{x})]$$

$$\approx -i\frac{\hbar}{m}\nabla_{\mathbf{x}}\delta^3(\mathbf{x}-\mathbf{x}'), \tag{7.25}$$

the last expression of which agrees with the commutation relation proposed by Landau [24]. Thus, we have shown that it is possible to rigorously define Landau's fluid velocity operator, if we start with the physically reasonable assumptions of finite momentum and finite boson number and take the continuous limit at the end of a calculation. If the continuous limit is taken, one does not have to use the $\mathbf{D}_{\mathbf{j}-\mathbf{j}'}$ defined in Eq. (7.19), and any $\mathbf{D}_{\mathbf{j}-\mathbf{j}'}$ that possesses the continuous limit given by Eq. (7.23) will suffice.

The fluid velocity is a physical quantity that can be measured optically. The bosonic fluid can act as a moving dielectric, in which a propagating light beam can acquire a phase shift proportional to the fluid velocity in the first order, due to the Fresnel drag effect [40]. Bosons may also reflect or scatter light, and the fluid velocity will shift the instantaneous frequency of the reflected or scattered light due to the Doppler effect. Thus, the fluid velocity and the optical instantaneous frequency are closely related physical quantities, and, as we have shown in this paper, can be described by the same theoretical formalism in the quantum regime.

VIII. CONCLUSION

In conclusion, we have proposed a quantum theory of optical phase and instantaneous frequency in the time domain. In the formalism, we have introduced an explicit optical bandwidth cutoff in order to reflect our experimental limitations, satisfy the slowly varying envelope approximation, and, most importantly, discretize time domain into discrete modes, the phases of which we know how to define and measure in principle. Guided by insights from classical estimation theory, we have suggested the use of homodyne phase-locked loops to perform angle demodulation, and the quantum limits are derived. We have also shown how the SNR enhancement effect of wideband angle modulation can be applied to optical sensing of position and velocity. Given the recent experimental advances in quantum-enhanced measurements [10,11,41] and the maturity of optical phase-locked loop technology [42], we expect our theoretical predictions to be experimentally realizable with current technology and relevant to future communication and sensing applications. Finally, we have applied the optical formalism to nonrelativistic bosons and we showed how Landau's fluid velocity operator can be defined rigorously, thus resolving a long-standing issue in quantum hydrodynamics. A more rigorous formulation of the current-algebra approach to quantum hydrodynamics based on our theory can be envisaged.

ACKNOWLEDGMENTS

This work is financially supported by the W. M. Keck Foundation Center for Extreme Quantum Information Theory.

APPENDIX A: ALGEBRA IN THE DISCRETE TIME DOMAIN

For convenience we adopt the following simplified notations to describe algebra in the discrete time domain. Boldface lowercase letters denote vectors in the discrete time domain,

$$\boldsymbol{a} \equiv \{\ldots, a_j, a_{j+1}, \ldots\}. \tag{A1}$$

Multiplication and division of components of two vectors are written implicitly,

$$\boldsymbol{ab} \equiv \{\ldots, a_j b_j, a_{j+1} b_{j+1}, \ldots\}, \tag{A2}$$

$$\frac{\boldsymbol{a}}{\boldsymbol{b}} \equiv \left\{\ldots, \frac{a_j}{b_j}, \frac{a_{j+1}}{b_{j+1}}, \ldots\right\}. \tag{A3}$$

A vector of functions of each component of $\boldsymbol{a}$ is written as a function of the vector,

$$f(\boldsymbol{a}) \equiv \{\ldots, f(a_j), f(a_{j+1}), \ldots\}, \tag{A4}$$

while a function of all components is written with square brackets,

$$f[\boldsymbol{a}] \equiv f(\ldots, a_j, a_{j+1}, \ldots). \tag{A5}$$

The dot product of two vectors is defined as

$$\boldsymbol{a}\cdot\boldsymbol{b} \equiv \sum_j a_j b_j. \tag{A6}$$

The tensor product of two vectors is

$$(\boldsymbol{a}\otimes\boldsymbol{b})_{jk} = a_j b_k. \tag{A7}$$

A matrix A_{jk} is written as boldface and uppercase $\boldsymbol{A}$. The transpose of a matrix is defined as

$$(\boldsymbol{A}^T)_{jk} \equiv A_{kj}. \tag{A8}$$

Dot products of a matrix and a vector are

$$(\boldsymbol{A}\cdot\boldsymbol{b})_j \equiv \sum_k A_{jk} b_k, \quad (\boldsymbol{b}\cdot\boldsymbol{A})_j \equiv \sum_k b_k A_{kj}. \tag{A9}$$

Multiplication of two matrices is

$$(\boldsymbol{A}\cdot\boldsymbol{B})_{jk} \equiv \sum_l A_{jl} B_{lk}. \tag{A10}$$

The inverse of a matrix, if it exists, is $\boldsymbol{A}^{-1}$,

$$\boldsymbol{A}\cdot\boldsymbol{A}^{-1} = \boldsymbol{A}^{-1}\cdot\boldsymbol{A} = \boldsymbol{I}, \tag{A11}$$

where $I_{jk} = \delta_{jk}$ is the identity matrix.

APPENDIX B: BROADBAND SQUEEZED VACUUM

We shall study the statistics of the squeezed vacuum [19,43] in the interaction picture. For simplicity, we assume that the squeezing spectrum is uniform and has a bandwidth of B_s. Starting with the vacuum quantum state, the output annihilation operator in the frequency domain of a band-limited squeezed vacuum can be written as

$$\hat{a}(f) = \begin{cases} \mu \hat{a}_{\text{vac}}(f) + \nu \hat{a}^{\dagger}_{\text{vac}}(-f), & |f| < B_s/2, \\ \hat{a}_{\text{vac}}(f), & |f| \geqslant B_s/2, \end{cases} \tag{B1}$$

where μ and ν are parametric gain parameters that satisfy

$$|\mu|^2 - |\nu|^2 = 1, \tag{B2}$$

and $\hat{a}_{\text{vac}}(f)$ is the annihilation operator with vacuum state statistics. Performing the inverse Fourier transform on Eq. (B1),

$$\hat{a}_j \equiv \frac{1}{\sqrt{B}} \int_{-B/2}^{B/2} df \hat{b}(f) \exp(-i2\pi f t_j), \tag{B3}$$

$$\hat{a}_{\text{vac},j} \equiv \frac{1}{\sqrt{B}} \int_{-B/2}^{B/2} df \hat{a}_{\text{vac}}(f) \exp(-i2\pi f t_j), \tag{B4}$$

the discrete-time-domain operator for a squeezed vacuum is

$$\hat{\boldsymbol{a}} = \hat{\boldsymbol{a}}_{\text{vac}} + \Gamma \cdot [(\mu - 1)\hat{\boldsymbol{a}}_{\text{vac}} + \nu \hat{\boldsymbol{a}}^{\dagger}_{\text{vac}}], \tag{B5}$$

where $\Gamma_{jk} = \Gamma_{j-k}$ is a low-pass filter defined as

$$\Gamma_{j-k} \equiv \frac{1}{B} \int_{-B_s/2}^{B_s/2} df \exp[-i2\pi f(t_j - t_k)]. \tag{B6}$$

We define the quadrature operators as

$$\hat{\boldsymbol{x}}_0 \equiv \hat{\boldsymbol{a}} + \hat{\boldsymbol{a}}^{\dagger}, \quad \hat{\boldsymbol{y}}_0 \equiv -i(\hat{\boldsymbol{a}} - \hat{\boldsymbol{a}}^{\dagger}). \tag{B7}$$

The vacuum-state operators have the following statistics:

$$\langle \hat{\boldsymbol{a}}_{\text{vac}} \rangle = \langle \hat{\boldsymbol{a}}^{\dagger}_{\text{vac}} \rangle = 0, \tag{B8}$$

$$\langle \hat{\boldsymbol{a}}^{\dagger}_{\text{vac}} \otimes \hat{\boldsymbol{a}}_{\text{vac}} \rangle = 0, \quad \langle \hat{\boldsymbol{a}}_{\text{vac}} \otimes \hat{\boldsymbol{a}}^{\dagger}_{\text{vac}} \rangle = \boldsymbol{I}, \tag{B9}$$

which lead to the following covariance matrices:

$$\boldsymbol{K}_1 \equiv \langle \hat{\boldsymbol{x}}_0 \otimes \hat{\boldsymbol{x}}_0 \rangle = \boldsymbol{I} - (1 - |\mu + \nu^*|^2)\boldsymbol{\Gamma}, \tag{B10}$$

$$\boldsymbol{K}_2 \equiv \langle \hat{\boldsymbol{y}}_0 \otimes \hat{\boldsymbol{y}}_0 \rangle = \boldsymbol{I} - (1 - |\mu - \nu^*|^2)\boldsymbol{\Gamma}. \tag{B11}$$

To produce squeezing in the $\boldsymbol{y}_0$ quadrature, both μ and ν should be real and positive. Writing μ and ν in terms of the squeeze parameter r,

$$\mu = \cosh r, \quad \nu = \sinh r, \tag{B12}$$

the covariance matrices become

$$\boldsymbol{K}_1 = \boldsymbol{I} - [1 - \exp(2r)]\boldsymbol{\Gamma}, \tag{B13}$$

$$\boldsymbol{K}_2 = \boldsymbol{I} - [1 - \exp(-2r)]\boldsymbol{\Gamma}. \tag{B14}$$

The quadrature power spectral densities are

$$S_1(f) = \begin{cases} \exp(2r), & |f| < B_s/2, \\ 1, & |f| \geqslant B_s/2, \end{cases} \tag{B15}$$

$$S_2(f) = \begin{cases} \exp(-2r), & |f| < B_s/2, \\ 1, & |f| \geqslant B_s/2. \end{cases} \tag{B16}$$

If $\hat{\boldsymbol{x}}_0$ and $\hat{\boldsymbol{y}}_0$ pass through a low-pass filter $\boldsymbol{L}$ with bandwidth $b < B_s$, their variances become

$$\langle (\boldsymbol{L} \cdot \hat{\boldsymbol{x}}_0)^2 \rangle = \frac{b}{B} \exp(2r), \tag{B17}$$

$$\langle (\boldsymbol{L} \cdot \hat{\boldsymbol{y}}_0)^2 \rangle = \frac{b}{B} \exp(-2r), \tag{B18}$$

and their ratio is

$$\frac{\langle (\boldsymbol{L} \cdot \hat{\boldsymbol{y}}_0)^2 \rangle}{\langle (\boldsymbol{L} \cdot \hat{\boldsymbol{x}}_0)^2 \rangle} = \exp(-4r), \tag{B19}$$

which provides an estimate of the magnitude of the right-hand side of the threshold constraint given by Eq. (4.70), if we regard $\boldsymbol{L}$ as a bandpass filter with bandwidth b.

[1] A. J. Viterbi, *Principles of Coherent Communication* (McGraw-Hill, New York, 1966).

[2] H. L. Van Trees, *Detection, Estimation, and Modulation Theory, Part I* (Wiley, New York, 2001); *Detection, Estimation, and Modulation Theory, Part II: Nonlinear Modulation Theory* (Wiley, New York, 2002).

[3] L. W. Couch, *Digital and Analog Communication Systems* (Prentice Hall, Englewood Cliffs, NJ, 2001).

[4] See, for example, A. Madjar, IEEE Trans. Microwave Theory Tech. **42**, 801 (1994); R. F. Kalman, J. C. Fan, and L. G. Kazovsky, J. Lightwave Technol. **12**, 1263 (1994); S. Betti, G. De Marchis, and E. Iannone, *Coherent Optical Communications Systems* (Wiley, New York, 1995); L. G. Kazovsky, G. Kalogerakis, and W.-T. Shaw, J. Lightwave Technol. **24**, 4876 (2006).

[5] Y. Yamamoto and H. A. Haus, Rev. Mod. Phys. **58**, 1001 (1986); C. M. Caves and P. D. Drummond, *ibid.* **66**, 481 (1994).

[6] H. A. Haus, *Electromagnetic Noise and Quantum Optical Measurements* (Springer-Verlag, Berlin, 2000).

[7] H. P. Yuen, in *Quantum Squeezing*, edited by P. D. Drummond and Z. Ficek (Springer-Verlag, Berlin, 2004), Chap. 7.

[8] See, for example, C. M. Caves, Phys. Rev. D **23**, 1693 (1981); R. S. Bondurant and J. H. Shapiro, *ibid.* **30**, 2548 (1984); B.

Yurke, S. L. McCall, and J. R. Klauder, Phys. Rev. A **33**, 4033 (1986); K. W. Leong and J. H. Shapiro, Opt. Commun. **58**, 73 (1986); S. L. Braunstein, A. S. Lane, and C. M. Caves, Phys. Rev. Lett. **69**, 2153 (1992); S. L. Braunstein, *ibid.* **69**, 3598 (1992); M. J. Holland and K. Burnett, *ibid.* **71**, 1355 (1993); J. H. Shapiro, Phys. Scr., T **T48**, 105 (1993); J. Jacobson, G. Bjork, I. Chuang, and Y. Yamamoto, Phys. Rev. Lett. **74**, 4835 (1995); Z. Y. Ou, Phys. Rev. A **55**, 2598 (1997); P. Kok, S. L. Braunstein, and J. P. Dowling, J. Opt. B: Quantum Semiclassical Opt. **6**, S811 (2004).

[9] J. H. Shapiro, S. R. Shepard, and N. C. Wong, Phys. Rev. Lett. **62**, 2377 (1989); J. H. Shapiro and S. R. Shepard, Phys. Rev. A **43**, 3795 (1991).

[10] V. Giovannetti, S. Lloyd, and L. Maccone, Science **306**, 1330 (2004); Phys. Rev. Lett. **96**, 010401 (2006).

[11] B. L. Higgins *et al.*, Nature (London) **450**, 393 (2007).

[12] V. B. Braginsky and F. Ya. Khalili, *Quantum Measurements* (Cambridge University Press, Cambridge, 1992).

[13] W. D. Bachalo, Int. J. Multiphase Flow **20**, 261 (1994).

[14] P. A. Oberg, Crit. Rev. Biomed. Eng. **18**, 125 (1990).

[15] L. Susskind and J. Glogower, Physics (Long Island City, N.Y.) **1**, 49 (1964); P. Carruthers and M. M. Nieto, Rev. Mod. Phys. **40**, 411 (1968).

[16] D. T. Pegg and S. M. Barnett, Phys. Rev. A **39**, 1665 (1989).

[17] J. W. Noh, A. Fougères, and L. Mandel, Phys. Rev. Lett. **67**, 1426 (1991); Phys. Rev. A **45**, 424 (1992); Phys. Rev. Lett. **71**, 2579 (1993); M. G. Raymer, J. Cooper, and M. Beck, Phys. Rev. A **48**, 4617 (1993).

[18] U. Leonhardt J. A. Vaccaro, B. Bohmer, and H. Paul, Phys. Rev. A **51**, 84 (1995).

[19] L. Mandel and E. Wolf, *Optical Coherence and Quantum Optics* (Cambridge University Press, Cambridge, 1995).

[20] C. W. Helstrom, *Quantum Detection and Estimation Theory* (Academic, New York, 1976).

[21] A. S. Holevo, *Probabilistic and Statistical Aspects of Quantum Theory* (North-Holland, Amsterdam, 1982).

[22] P. A. M. Dirac, Proc. R. Soc. London, Ser. A **114**, 243 (1927).

[23] P. W. Anderson, Rev. Mod. Phys. **38**, 298 (1966); F. Dalfovo *et al.*, *ibid.* **71**, 463 (1999); A. J. Leggett, *ibid.* **73**, 307 (2001).

[24] L. D. Landau, J. Phys. (USSR) **5**, 71 (1941).

[25] F. London, Rev. Mod. Phys. **17**, 310 (1945); H. Fröhlich, Physica (Amsterdam) **34**, 47 (1967); J. C. Garrison, H. L. Morrison, and J. Wong, J. Math. Phys. **11**, 630 (1970); D. H. Kobe and G. C. Coomer, Phys. Rev. A **7**, 1312 (1973).

[26] R. F. Dashen and D. H. Sharp, Phys. Rev. **165**, 1857 (1968); D. H. Sharp, *ibid.* **165**, 1867 (1968); R. Fanelli and R. E. Struzynski, *ibid.* **173**, 248 (1968); **182**, 363 (1969); D. J. Gross, *ibid.* **177**, 1843 (1969); D. D. H. Yee, *ibid.* **184**, 196 (1969); J. Grodnik and D. H. Sharp, Phys. Rev. D **1**, 1531 (1970); G. S. Grest and A. K. Rajagopal, Phys. Rev. A **10**, 1395 (1974).

[27] H. M. Wiseman, Phys. Rev. Lett. **75**, 4587 (1995); H. M. Wiseman and R. B. Killip, Phys. Rev. A **56**, 944 (1997); Phys. Rev. A **57**, 2169 (1998).

[28] D. W. Berry and H. M. Wiseman, Phys. Rev. A **63**, 013813 (2000).

[29] D. W. Berry and H. M. Wiseman, Phys. Rev. A **65**, 043803 (2002); Phys. Rev. A **73**, 063824 (2006).

[30] H. P. Yuen and J. H. Shapiro, IEEE Trans. Inf. Theory **IT-24**, 657 (1978); B. Huttner and S. M. Barnett, Phys. Rev. A **46**, 4306 (1992).

[31] J. H. Shapiro, Quantum Semiclassic. Opt. **10**, 567 (1998); M. Tsang, Phys. Rev. A **75**, 043813 (2007); **75**, 063809 (2007).

[32] A. L. Fetter and J. D. Walecka, *Quantum Theory of Many-Particle Systems* (Dover, Mineola, NY, 2003).

[33] K. L. Pregnell and D. T. Pegg, Phys. Rev. Lett. **89**, 173601 (2002); Phys. Rev. A **67**, 063814 (2003).

[34] J. G. Proakis and D. G. Manolakis, *Digital Signal Processing* (Prentice Hall, Englewood Cliffs, NJ, 1996).

[35] H. P. Yuen and J. H. Shapiro, IEEE Trans. Inf. Theory **26**, 78 (1980).

[36] D. F. Walls and G. J. Milburn, *Quantum Optics* (Springer-Verlag, Berlin, 1995).

[37] J. H. Shapiro and S. S. Wagner, IEEE J. Quantum Electron. **20**, 803 (1984).

[38] V. P. Belavkin, Rep. Math. Phys. **43**, A405 (1999); F. Verstraete, A. C. Doherty, and H. Mabuchi, Phys. Rev. A **64**, 032111 (2001); D. T. Pope, H. M. Wiseman, and N. K. Langford, *ibid.* **70**, 043812 (2004).

[39] B. Abbott *et al.*, Nucl. Instrum. Methods Phys. Res. A **517**, 154 (2004).

[40] U. Leonhardt and P. Piwnicki, Phys. Rev. A **60**, 4301 (1999).

[41] K. Goda *et al.*, Nat. Phys. **4**, 472 (2008).

[42] V. Ferrero and S. Camatel, Opt. Express **16**, 818 (2008).

[43] C. M. Caves and B. L. Schumaker, Phys. Rev. A **31**, 3068 (1985).